Molecular Dynamics Study of a Thermal Expansion Coefficient: Ti Bulk with an Elastic Minimum Image Method

Yakup Hundur[1*], Rainer Hippler[2] and Ziya B. Güvenç[3]

[1] *Department of Physics, Istanbul Technical University, Ayazaga, Istanbul, TR-34469 Turkey*
[2] *Institut für Physik, Ernst-Moritz-Arndt-Universität Greifswald,*
Domstraße 10a, D-17487 Greifswald, Germany and
[3] *Electronic and Communication Engineering, Çankaya University, Balgat, Ankara, TR-06530 Turkey*

Linear thermal expansion coefficient (TEC) of Ti bulk is investigated by means of molecular dynamics simulation. Elastic Minimum Image Convention of periodic boundary conditions is introduced to allow the bulk to adjust its size according to the new fixed temperature. The TEC and the specific heat of Ti are compared to the available theoretical and experimental data.

INTRODUCTION

Titanium is not present in pure form in the nature, and its composites have different thermal expansion coefficients (TEC) [1]. Determining the TEC values may help to guess the composition. For expansion simulations, various Molecular Dynamics (MD) methods allowing for a volume change exist [2, 3]. Expansion is defined through a change of the bond length which may be determined with several methods, like the average length of the bulk diagonals [4]. For a more statistically dependable result, the mean distances between the atoms in the bulk are calculated in this work. Expansion of the sample requires elasticity of the periodic boundary conditions (PBC), but the PBC and its minimum image convention use fixed box lengths in the simulation [2]. Therefore, elastic minimum image convention (EMIC) of the PBC is introduced. It resembles Berendsen's barostat method. However, Berendsen's method allows only isotropic changes in the volume of the simulation box [2], while the EMIC method allows change of the shape as well as its size. For the present purpose correctness of the elastic constants and phonon frequencies are important. The recent many-body potentials such as Finnis-Sinclair, Gupta, and Glue potentials and embedded atom method cannot reproduce all elastic constants correctly [5], while Lennard-Jones potential (LJ) [6] give good results [7] for Ti. Hence the LJ potential is employed into our temperature scaled isoenergetic and isobaric MD codes [4]. Relaxation runs of the bulk Ti have been performed by using this code. The Verlet integration algorithm [8] is used, since it allows for time-reversible actions [9].

*To whom correspondence should be addressed. E-mail: hundur@itu.edu.tr.

ELASTIC MINIMUM IMAGE CONVENTION (EMIC)

The EMIC method is used to adjust the simulation box lengths to the temperature changes during a run [4]. The entire simulation time t_{tot} is divided into nb number of time-blocks Tb, each consisting of m time-steps ts, with δt time step size (tss), which can be expressed as $t_{tot} = nb \times Tb$ and $Tb = m \times \delta t$.

The mean bond length MBL is calculated from

$$MBL = \frac{1}{C(N,2)} \sum_{i>j}^{N} r_{ij} \tag{1}$$

where N, C and r_{ij} are the total number of atoms, combination of N by 2 and pair distance in the simulation cell, respectively. The changes in MBL are reflected directly to the box length. Although, temperature scaling is applied after each Tb, EMIC is only applied after some number of Tb, let's call $nscb$. Therefore, EMIC is applied at every ecb time interval, i.e., $ecb = nscb \times Tb$, where $nscb = [1\text{--}100]$. The system temperature fluctuates freely during each Tb, while the MBL differences accumulate and the system tries to reach an equilibrium during each ecb [4]. In this way, the system also fulfils ergodicity. The difference in MBL during the kth and $(k-1)^{th}$ ecb is

$$\begin{aligned}\Delta MBL_{k,k-1} &= \left(\frac{1}{nscb} \sum_{i=1}^{nscb} \overline{MBL_i}\right)_k \\ &\quad - \left(\frac{1}{nscb} \sum_{i=1}^{nscb} \overline{MBL_i}\right)_{k-1} \\ &= \langle\overline{MBL}\rangle_{ecb(k)} - \langle\overline{MBL}\rangle_{ecb(k-1)}\end{aligned} \tag{2}$$

where $\overline{MBL_i}$ is the average during the ith Tb, and the terms on the right hand side are the MBL averages at the kth and $(k-1)^{th}$ ecb. An effective MBL average at the kth ecb is obtained by multiplication of $\Delta MBL_{k,k-1}$ with an adjustable parameter p as

$$\langle\overline{MBL}\rangle_{ecb(k)}^{eff} = p\,\Delta MBL_{k,k-1} + \langle\overline{MBL}\rangle_{ecb(k-1)}^{eff} \tag{3}$$

where $0 < p \leq 1$. Note that Eq. 3 becomes Eq. 2 if $p = 1$. Finally, the box length of the EMIC in the

x-direction from k^{th} to $(k+1)^{th}$ ecb is

$$BoxLx_{ecb(k+1)} = BoxLx_{ecb(k)} \frac{\langle \overline{MBL} \rangle^{eff}_{ecb(k)}}{\langle \overline{MBL} \rangle^{eff}_{ecb(k-1)}} . \quad (4)$$

Similar equations hold for the other directions. Since the radial MBL averages are reflected to each of the directions as in Eq. 3, the initial shape of the bulk is forced remain to unchanged. However, the real lattice may not expand with the same rate along each of the Cartesian directions [10, 11]. Therefore Eq. 3 is reformulated for each coordinate separately as

$$\langle \overline{MBLx} \rangle^{eff}_{ecb(k)} = p \, \Delta MBLx_{k,k-1} + \langle \overline{MBLx} \rangle^{eff}_{ecb(k-1)} \quad (5)$$

Similarly, Eq. 4 is also reformulated for each direction separately as

$$BoxLx_{ecb(k+1)} = BoxLx_{ecb(k)} \frac{\langle \overline{MBLx} \rangle^{eff}_{ecb(k)}}{\langle \overline{MBLx} \rangle^{eff}_{ecb(k-1)}} \quad (6)$$

Values of m in a Tb should be chosen as large as possible for the numerical convergence of the physical quantities, in order to reduce non-physical effects [2]. Hence, several test runs are required to determine the parameters m, $nscb$, and p.

SIMULATION

The conventional α–Ti has hcp structure. The characteristics of a hcp cell are determined by proportionality of simple cell sizes c/a. This ratio and the binding energy parameter ε_0 are taken as 1.62073 and 0.20154 eV when producing the LJ potential for Ti [7], while the recent experimental c/a value is 1.601 [12]. The unit cell sizes are $a = 2.94055$ Å and $c = 4.76583$ Å for LJ potential compared to $a = 2.953$ Å and $c = 4.729$ Å from experiment. The bulk sample in the simulation is prepared using the former set of constants. A safe cut-off radius for the interactions is chosen as $2.8\,\sigma$ ($\sigma = 2^{1/6}r_0$) [2], where the bond length r_0 is 2.96292 Å [7]. Since the box length should be equal or greater than twice the cut-off radius [2], the smallest possible sample having 389 Ti atoms with a lattice size of $6a \times 6b \times 4c$, i.e., $17.718 \times 17.718 \times 18.916$ Å³ is constructed.

Simulations have been carried out for the temperature range 100–400 K, in steps of 100 K. Quantum effects on the specific heat become important at low temperatures [13]; as these effects are not included in the binary potentials [14], the lower temperature was chosen as 100 K. The higher temperature limit is set near the Debye's temperature, since the binary potentials require modifications for the higher temperatures [3]. The final velocities and coordinates of the previous run are used as the initial conditions for the next run, i.e., those of the 200

K are used as the initial values for the 300 K run, and so on. At each temperature two different simulations were performed one after the other. Firstly, the bulk is run under constant pressure by using the EMIC boundary conditions to adjust the bulk sides. After that, the code is run by using PBC under this constant volume.

The time averaged temperature over each Tb is calculated from

$$T(K) = \frac{2\langle E_{kin} \rangle}{(3N-6)k_B} \quad (7)$$

where $\langle E_{kin} \rangle$ is the time averaged kinetic energy of the atoms, N is the number of atoms in the sample, and k_B is the Boltzmann constant. Hence, the simulation temperature is the average over all $T(K)$ values.

A number of runs have been made to find the right parameters. The tss and Tb are varied between 0.2–2 fs ($1\text{fs} = 10^{-15}$ sec) and 10–100 tss, respectively. The total number of time steps lie within the range of 163,000–2,002,000 and the resulting total run times are varied in between 18,700 fs and 402,000 fs. The coefficient p of the effective MBL differences is used as 0.5–1 in order to let the system change smoothly. Otherwise, if p is taken equal to 1, a sudden change in the periodic box size may lead to excess energy at some particles.

Firstly, average bond differences $\Delta MBL_{k,k-1}$ are distributed proportionally, according to c/a ratio, to each of the Cartesian directions of the EMIC box by Eqs. 3 and 4. Therefore the shape of the bulk is enforced to remain globally unchanged. However, this brutal sharing brought the problem of exceeding force accumulation, and the problem of stability at 300 K and 400 K. Using small time step sizes has solved the problem of 300 K, but not at the higher temperatures. Then, $\Delta MBL_{k,k-1}$ is shared to each Cartesian coordinate separately, and the bulk is reconstructed in each direction independently (Eqs. 5 and 6). This causes accidental image conventions of the coordinates after some number of time intervals. In order to avoid these and to reach numerical convergence of the physical quantities, some number of runs have been done to determine the run parameters.

Together with the temperature of the bulk, coordinates of the atoms along each of the Cartesian directions, kinetic, potential and total energies of the atoms are calculated. Fluctuations on all these quantities, specific heat and thermal expansion coefficients are obtained.

The linear thermal expansion coefficient (TEC) is defined as

$$\alpha = \frac{1}{L_0} \frac{\Delta L}{\Delta T} \quad (8)$$

where L_0, ΔL, and ΔT are the initial length, change of length and change of temperature, respectively. In practice, L is calculated with various methods throughout the entire run. In this work, MBL and MBL_0 are used in place of L and L_0, respectively.

Heat capacity can be observed by doing a series of simulations at different temperatures with corresponding constant volumes. It can be calculated in each run separately by using temperature or energy fluctuations. Various authors have offered similar forms for the calculation of heat capacity [2, 9]. It is defined through kinetic energy fluctuations for the microcanonical ensembles by Lebowitz et al. [15] as

$$C_V = \frac{3}{2} N k_B \left(1 - \frac{2}{3} \frac{\sigma^2(KE)}{N k_B T^2} \right)^{-1} \qquad (9)$$

where $\sigma^2(KE)$ is mean square deviation of the kinetic energy throughout the entire run.

RESULTS AND DISCUSSIONS

Shape of the Bulk

Small changes on the coordinates of the bulk atoms are observed. Typical bond length changes are about 0.01–0.04 Å (0.34–1.35% of $T = 0$ K bond length). The centre of mass is unchanged during the simulations. Between 100–300 K the shape of the bulk remains more or less unchanged. However, at 400 K the resulting bulk has a shape anomaly like in the experiments where the expansion of the bulk varies in different directions [10, 11]; the difference of the c/a value after the 400 K simulation is roughly 0.4% in comparison to its $T = 0$ K value.
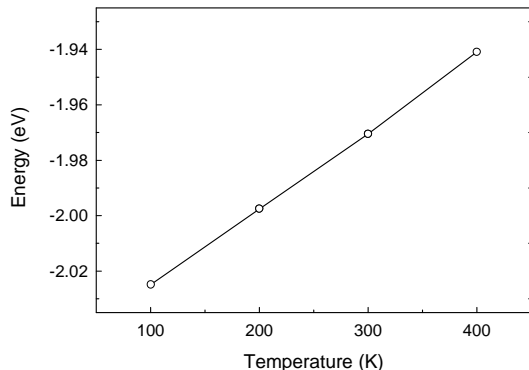

FIG. 1: Caloric curve of the Ti–389 bulk obtained by the simulation.

Specific Heat Capacity

The temperature development at different total energies, resulted from the simulation, is shown in Fig. 1. A linear behaviour and a small increase are seen by increasing the temperature, although the total energies at each temperature are constant with small fluctuations. The maximum fluctuations are roughly 10^{-5} eV as expected

[2]. Moreover, the temperature values are observed to be certain within [0.004, 0.047] K error. The heat capacities are observed by using the method explained in the preceding section. These are calculated at each temperature using Eq. 9. The results are compared to the available experimental data [16, 17] in Fig. 2. There exists a good agreement. The Maximum difference occurs at 100 K as of 17%. The mean square deviation of the kinetic energy of the atoms in Eq. (11) is taken as 1s, if it were taken as 2s which covers the 95% of the region- they would have certainly covered the whole experimental values.
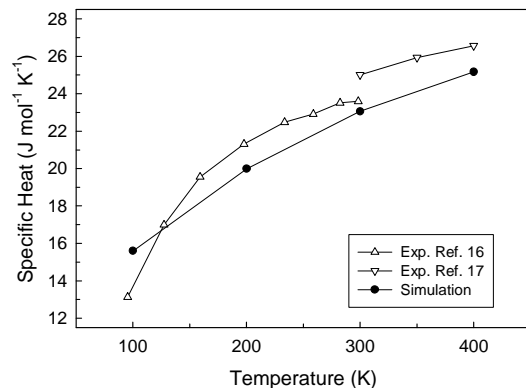

FIG. 2: Comparison of this simulation and experimental results for the specific heat capacities of Ti. ● present simulation; △, experiment, Ref. [16]; ▽, experiment, Ref. [17].
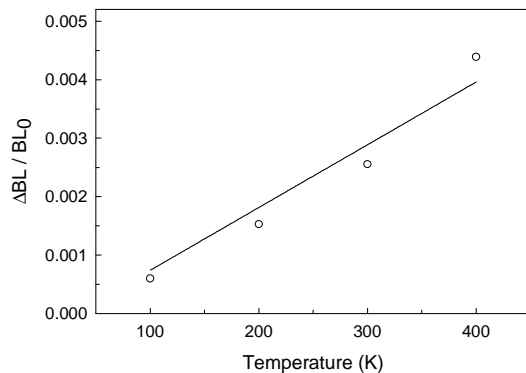

FIG. 3: The calculated rate of change of the mixed bond length values against temperature. The solid curve represents the linear best fit.

Thermal Expansion Coefficient

The linear thermal expansion coefficient of the Ti is calculated from Eq. 8 using the MBL. The MBL varies with the temperature of the bulk. The temperature dependence of the relative MBL change, $\Delta MBL/MBL_0$, is shown in Fig. 3, where MBL_0 is the mixed bond length at $T = 0$ K. It is important to note that the $T = 0$ K

value is only a reference point and not a simulation result. As seen, the curve exhibits a nearly linear increase in this temperature range.

TABLE I: Experimental and our simulation results (in units of 10^{-6}/K) for the linear thermal expansion coefficient of Ti as function of temperature T.

T (K)	MD	Experiments
100	4.48	—
200	7.73	—
300	8.50	8.35 (a) 8.5 (b) 8.6 (c) 11.9 (d)
400	10.99	9.32 (b)
300–400	9.74 (f)	8.7 (e)

(a) T= 298.15 K, Ref. [18]
(b) Ref. [11]
(c) T= 298.15 K, Ref. [12]
(d) T= 23 ^{o}C (296.15 K), Ref. [19]
(e) T= 20–100 ^{o}C (293.15–393.15 K), Ref. [18]
(f) Mean value of simulations between $T = 300$–400 K.

The calculated TEC of the Ti values are tabulated in Table I together with the available experimental results. We could not find any experimental TEC value below 300 K to compare with our simulation results. The experimental results at 300 K [11, 12, 18, 19] show noticeable irregularity. One of them perfectly matches with the simulation result. At 400 K, the simulation result of 10.99×10^{-6}/K differs by 18% from the experimental result of Ref. [11]. The difference is smaller in the 300–400 K range, 12%, where the simulation and experimental results are 9.74×10^{-6}/K and 8.7×10^{-6}/K, respectively.

SUMMARY

Isobaric and isoenergetic MD simulations have been performed with Verlet algorithm. The LJ potential parameters of Yamamoto-Kagawa-Doyama is used for the Ti-Ti interactions. A Ti–389 sample is produced by using the same lattice constants of this potential. The elastic minimum image convention of the periodic boundary conditions is set to enable the elasticity of the bulk. Constant pressure, and isoenergetic simulations have been done, one after the other. Specific heat and linear TEC of Ti are calculated between 100 K and 400 K. The lower temperature is determined to reduce the quantum effects [13]. And the upper limit is set to the Debye's temperature since the binary potentials require modifications for the higher temperatures [3]. The calculated TEC value at 300 K matches perfectly with one of the experiment,

while the highest difference occurred as 18% at 400 K. Furthermore, observed path of the specific heat in the simulation has a similar path with the experiments as shown in Fig. 2. Numerical convergence problems at both temperature limits are observed in the simulation. Solving the high temperature problems will be our future work to clarify the behaviour in this regime.

[1] Williams J J, Kramer M J and Akinc M Aug 2000 J. Mater. Res. 15 8
[2] Allen M P and Tildesley D J 1987 Computer Simulation of Liquids (Oxford: Clarendon Press) chap 7 pp232-8, chap 1 pp24-9, chap 9 p29, chap 2 p53
[3] Wu E Y 1990 J. Phys.: Condens. Matter 2 9335-9344
[4] Hundur Y (PhD thesis) 2003 Determination of the Thermal Expansion Coefficient of Titanium, and Sputtering Process by Molecular Dynamics Simulation (University of Greifswald) (unpublished)
[5] Pasianot R and Savino E J 1992 Phys. Rev. B 45 12704
[6] Lennard-Jones J E 1924 Proc. R. Soc. Lond. 106A 441
[7] Yamamoto R, Kagawa S and Doyama M 1980 Titanium 80 773-780
[8] Verlet L 1967 Phys. Rev. 159 98
[9] Frenkel D and Smit B 1996 Understanding Molecular Simulation, From Algorithms to Applications (San Diego: Academic Press) chap 4 p64, chap 4 p75
[10] de Wette F W in Gehlen P C, Beeler Jr J R and Jaffee R I (eds.) 1972 Interatomic Potentials and Simulation of Lattice Defects (New York: Plenum Press) p661
[11] Russell A M and Cook B A 1997 Scripta Materialia Vol.37 10 1461-1467
[12] Lide D R (ed.) 1999 CRC Handbook of Chemistry and Physics 80th edition (Boca Raton, Florida: CRC Press) p12-194
[13] Kittel C 1973 Einführung in die Festkörperphysik (München Wien: R Oldenburg John Wiley) chap 6 p246 (in German)
[14] Rohlf J M 1994 Modern Physics from α to Z0 (Wiley) in http://hyperphysics.phy-astr.gsu.edu/
[15] Lebowitz J L, Percus J K and Verlet L 1967 Phys. Rev. 153 250-4
[16] Rao R R and Rajput A 1979 Phys. Rev. B 19 3323
[17] Stassis C, Arch D, Harmon B N and Wakabayashi N 1979 Phys. Rev. B 19 181
[18] Carderelli F 1999 Materials Handbook, A Concise Desktop Reference (London, Berlin, Heidelberg: Springer Verlag) chap 3 pp118, 126
[19] Bever M B (ed.) 1986 Encyclopedia of Materials Science and Engineering (New York: Pergamon Press)